



HAL
open science

Are the fluorescent properties of the cyan fluorescent protein sensitive to conditions of oxidative stress?

Luis A.J. Alvarez, Chantal Houee Levin, Fabienne Merola, Tania Bizouarn, H el ene Pasquier, Laura Baciou, Filippo Rusconi, Marie Erard

► **To cite this version:**

Luis A.J. Alvarez, Chantal Houee Levin, Fabienne Merola, Tania Bizouarn, H el ene Pasquier, et al.. Are the fluorescent properties of the cyan fluorescent protein sensitive to conditions of oxidative stress?. Photochemistry and Photobiology, 2010, 10.1111/j.1751-1097.2009.00617.x . hal-04058486

HAL Id: hal-04058486

<https://universite-paris-saclay.hal.science/hal-04058486>

Submitted on 4 Apr 2023

HAL is a multi-disciplinary open access archive for the deposit and dissemination of scientific research documents, whether they are published or not. The documents may come from teaching and research institutions in France or abroad, or from public or private research centers.

L'archive ouverte pluridisciplinaire **HAL**, est destin ee au d ep ot et  a la diffusion de documents scientifiques de niveau recherche, publi es ou non,  emanant des  tablissements d'enseignement et de recherche fran ais ou  trangers, des laboratoires publics ou priv es.

Are the Fluorescent Properties of the Cyan Fluorescent Protein Sensitive to Conditions of Oxidative Stress?

Luis Alvarez¹, Chantal Houée Levin¹, Fabienne Merola¹, Tania Bizouarn¹, Hélène Pasquier¹, Laura Baciou¹, Filippo Rusconi² and Marie Erard^{*1}

¹Laboratoire de Chimie Physique, Université Paris-Sud, Orsay Cedex, France

²Laboratoire de biophysique, Muséum national d'Histoire naturelle, rue Cuvier, Paris, France

Received 6 May 2009, accepted 5 July 2009, DOI: 10.1111/j.1751-1097.2009.00617.x

ABSTRACT

1The modifications induced by reactive oxygen species (ROS) on fluorescent proteins (FPs) may have important implications for live cell fluorescence imaging. Using quantitative γ -radiolysis, we have studied the ROS-induced biochemical and photophysical perturbations on recombinant cyan fluorescent protein (CFP). After oxidation by the $\cdot\text{OH}$ radical, the protein displays a modified RP-HPLC elution profile, while the CFP fluorescence undergoes pronounced decreases in intensity and lifetime, without changes in its excitation and emission spectra. Meanwhile, the Förster resonant energy transfer (FRET) between the single W^{57} and the chromophore remains unperturbed. These results rule out a direct oxidation of the CFP chromophore and of W^{57} as well as major changes in the protein 3D structure, but show that new fluorescent forms associated to a higher level of dynamic quenching have been generated. Thus, strict *in situ* controls are required when CFP is to be used for FRET studies in situations of oxidative activity, or under strong illumination.

INTRODUCTION

For nearly 15 years now, the many variants and homologs of the green fluorescent protein from *Aequorea victoria* (*wtGFP*) have revolutionized the mechanistic investigation of cellular processes by live cell imaging, flow cytometry and high-throughput bioassays (1–3). In addition to protein localization and trafficking, GFP-like proteins (called FPs, for short, in the present report) allow a detailed analysis of cell chemistry, *e.g.* for monitoring specific protein–protein interactions, enzymatic activities or second messenger signaling (3). Chemical sensing requires a thorough knowledge of the FPs photophysical responses to its local microenvironment. While some attention has been paid to the effects of either pH (4–6), chloride ions (7,8) or refractive index (9), another important aspect is the possible local production of reactive oxygen species (ROS) by living cells, which are generally responsible for the so-called oxidative stress. Indeed, ROS are produced in a number of biological pathways, ranging from signal transduction to apoptosis (10). The dynamics of pathogen phago-

cytosis, a phenomenon correlated with high levels of ROS production by enzymatic systems like NADPH oxidase and nitric oxide synthase, is currently being investigated with the help of FPs (11,12), while there has been a recent push to develop new members of the FP family as specific oxidation sensors (13–16). Moreover, photochemistry under oxygenic conditions originates mostly from the side-production of ROS from the singlet or triplet fluorophore excited states (17). The amount of ROS produced upon FP illumination can be so high that some FP variants have been developed as photosensitizers (18). In FPs, as in organic chromophores, these reactions can lead either to photobleaching or photoconversion. These reactions are responsible of crucial issues in modern fluorescence microscopy if they are not well mastered (1). But, on the other hand, they have, in some case, given birth recently to innovative imaging techniques like super-resolution optical microscopy (19).

Up until now, only a few groups have studied the consequences of ROS exposure on FPs (13,20–22). Reaction with the superoxide anion modifies the electrophoretic behavior of *wtGFP* without changing its absorption and fluorescent properties (20). Several oxidants involved in pathogen killing or inflammatory processes such as HClO , ONOO^- and $\text{NO}_2\cdot$ were shown to quench GFP fluorescence very effectively (21,22). GFP oxidized by HClO displays decreased chromophore absorption and fluorescence, showing that in this particular case, the chromophore itself is modified (22). On the other hand, Tsourkas *et al.* (13) explored the reactivity of some FPs (cyan fluorescent protein or CFP, yellow fluorescent protein or YFP, **2**GFP and DsRed) with the heme-peroxidase/ H_2O_2 system and found markedly different responses depending on the protein. Therefore, each FP has a specific reactivity and thus needs a dedicated study. The CFP, in combination with its partner, the YFP, is widely used as a biophysical probe in biochemical assays and imaging techniques based on Förster resonant energy transfer (FRET). Knowledge of the ROS sensitivity of CFP is particularly crucial, as FRET techniques require a quantification of the donor fluorescence, through *e.g.* (1) the variations of the CFP fluorescence lifetime or (2) the variations of its fluorescence intensity before and after thorough acceptor photobleaching (23). Moreover, a detailed knowledge of the CFP reactions with ROS and their consequences on its photophysical properties will improve the understanding of the

*Corresponding author email: marie.erard@lcp.u-psud.fr (Marie Erard)

© 2009 The Authors. Journal Compilation. The American Society of Photobiology 0031-8655/09

1 structure–photophysical properties relationship not only in the
2 CFP itself but also for other FP homologs of the GFP.

3 In this study, we have analyzed the biochemical and
4 photophysical perturbations induced by controlled amounts
5 of hydroxyl ($\bullet\text{OH}$) and/or superoxide anion ($\text{O}_2^{\bullet-}$) free
6 radicals, produced by γ -radiolysis of aqueous solutions of
7 recombinant CFP. Indeed, water γ -radiolysis combined with
8 the use of scavengers is a well controlled, selective and
9 quantitative method to produce free radicals (24). We find a
10 significant dynamic quenching of the CFP fluorescence asso-
11 ciated with $\bullet\text{OH}$ oxidation, without major perturbation of the
12 absorption and fluorescence spectral shapes. These effects bear
13 some resemblance with the previously reported consequences
14 of increasing temperature (6) and strong illumination (25) on
15 CFP fluorescence.

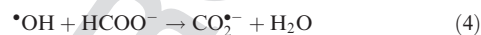
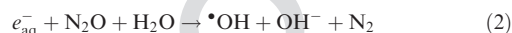
16 MATERIALS AND METHODS

17 *CFP purification and His-tag cleavage.* Production and purification of
18 His-tagged recombinant CFP was performed using TOP10 bacterial
19 cells. Competent cells were transformed with the pHis-CFP vector (a
20 generous gift from Dr. R. Grailhe, Institut Pasteur, Korea) (6).
21 A volume of 1.5 L of Luria–Bertani (LB) medium containing
22 ampicillin ($100\ \mu\text{g mL}^{-1}$) was inoculated with a 25 mL starter culture
23 that was grown overnight. Protein production was induced
24 ($\text{OD}_{600}\sim 0.6$) using isopropyl- β -D-thio-galactopyranoside (IPTG,
25 1 mM). After 18 h of culture at 30°C , bacteria were harvested by
26 centrifugation and frozen. The cells were resuspended in lysis buffer
27 (30 mL; 50 mM Tris–HCl, 5 mM 2-mercaptoethanol, 1 mM PMSF and
28 $0.02\ \text{mg mL}^{-1}$ DNase), and sonicated. The cell debris were removed by
29 centrifugation at 40 000 rpm for 1 h 30 at 6°C . The supernatant was
30 filtered with a $0.22\ \mu\text{m}$ filter and diluted by a factor 2 with phosphate
31 buffer (30 mM NaH_2PO_4 , 700 mM NaCl and 30 mM imidazole, pH
32 7.5). The solution was then applied to a column containing Ni–NTA
33 agarose (15 mL; Sigma) for 1 h. The column was then washed (30 mM
34 NaH_2PO_4 , 100 mM NaCl and 10 mM imidazole, pH 7.5) and the
35 protein was eluted (30 mM NaH_2PO_4 , 100 mM NaCl and 150 mM
36 imidazole, pH 7.5). The purified fusion protein His-CFP was further
37 concentrated and the elution buffer was replaced by the cleavage buffer
38 (50 mM Tris–HCl, 0.5 mM EDTA and 1 mM DTT, pH 8). The cleavage
39 of the His-tag was performed at room temperature during 5 h with a
40 TEV protease (see below) (26; further details are provided in
41 Supporting Information). The amount of protease has been estimated
42 with the absorbance of the protein solutions at 280 nm. The optimum
43 E/S ratio was estimated to be 1/20 by measuring absorbance at
44 280 nm. Full cleavage purification was monitored by SDS–PAGE (the
45 protein band shifts from 29 to 27 kDa apparent mass; data not
46 shown). A Ni–NTA agarose column with no affinity to the cleaved
47 enzyme was used for His-tag and protease removal from the CFP solution.
48 Before storage at -20°C , the CFP solution was dialyzed against 30 mM
49 phosphate, pH 7.5, for further experiments. The concentration of the CFP
50 was measured by absorption ($\epsilon_{434\ \text{nm}} = 32\ 500\ \text{mol}^{-1}\ \text{L cm}^{-1}$) (27).

51 *TEV protease purification.* For the cleavage of the CFP His-tag we
52 used the His-TEV(S219V) protease. This mutant is resistant to auto-
53 inactivation and is also a slightly more efficient catalyst than the wild
54 type enzyme (26). This His-tagged recombinant TEV protease was
55 prepared using the bacterial BL21 strain. Competent cells were
56 transformed with the pRK973 vector (Addgene). Cells were grown at
57 37°C in LB medium containing ampicillin ($100\ \mu\text{g mL}^{-1}$) and chloroam-
58 phenicol ($25\ \mu\text{g mL}^{-1}$). When the cells reached mid log phase
59 ($\text{OD}_{600}\sim 0.6$), IPTG was added to a final concentration of 1 mM and
60 the temperature was reduced to 30°C . After 5 h of induction, the cells
61 were collected by centrifugation and frozen at -20°C . The cell pellet
was resuspended in lysis buffer ($10\ \text{mL g}^{-1}$ of wet cell paste, 50 mM
 NaH_2PO_4 , 100 mM NaCl, 10% glycerol, and 25 mM imidazole, pH 7.5)
and the cells were lysed by sonication. Then a solution of polyethy-
leneimine (5% in water, adjusted to pH 7.9 with HCl) was added to the
lysate with a final concentration of 0.1%. After an immediate mixing
by inversion the solution was centrifuged at $15\ 000\ g$ for 30 min. The
supernatant was then loaded on a Ni–NTA agarose column (15 mL;

Sigma) equilibrated with lysis buffer. After washing, the TEV protease
was eluted with a buffer containing imidazole (50 mM NaH_2PO_4 ,
100 mM NaCl, 10% glycerol and 300 mM imidazole, pH 7.5). The
appropriate fractions were pooled and the protein was stored until use at
 -20°C in 50 mM phosphate, 100 mM NaCl and 10% glycerol, pH 7.5.

Radical production and radiolysis. The well-known method of
scavengers (24) allows a quantitative production of free radicals by
stationary γ -radiolysis according to the following reactions:



For instance in N_2O -saturated aqueous solutions, radiolysis
creates $\bullet\text{OH}$ radicals with a radiation chemical yield (G) equal to
 $0.55\ \mu\text{mol J}^{-1}$ (Eqs. 1 and 2) (24). In O_2 -saturated solutions and in
the presence of formate ions (HCOONa , 1 mM), Reactions 1 and
3–5 take place to form superoxide radical anions, $\text{O}_2^{\bullet-}$, with a
radiation chemical yield equal to $0.55\ \mu\text{mol J}^{-1}$. In air atmosphere
and without the help of other scavengers than O_2 , several reactions
take place (including Reactions 1 and 3), thus $\bullet\text{OH}$ and $\text{O}_2^{\bullet-}$
radicals are present simultaneously. The radiation chemical yields of
 $\text{O}_2^{\bullet-}$ and $\bullet\text{OH}$ were evaluated in this case by simulation to be 0.31
and $0.28\ \mu\text{mol J}^{-1}$, respectively (28). γ -Irradiations were carried out
using the panoramic ^{60}Co γ -source IL60PL Cis-Bio International
(France) in the University Paris-Sud (Orsay, France). The dose rate
was determined by Fricke dosimetry (24) and kept constant at
 $4.5\ \text{Gy min}^{-1}$. Samples were purged gently under agitation without
bubbling with N_2O or O_2 for 60 min before irradiation. Sodium
formate was of the highest quality available (Prolabo Normatom or
Merck Suprapure). Oxygen was delivered by ALPHA GAZ. Its
purity is higher than 99.99%. Water was purified using a Millipore
system (resistivity $18.2\ \text{M}\Omega$).

All irradiations were performed at room temperature. The CFP
concentration for irradiations was $5\ \mu\text{M}$ at neutral pH (30 mM
phosphate buffer, pH 7.5, sample volume $100\text{--}500\ \mu\text{L}$). The doses
applied ranged from 20 to 400 Gy. A more significant parameter is the
concentration ratio $[\text{radicals}]/[\text{CFP}]$, which is proportional to the dose:
 $[\text{radicals}] = \text{dose} \times G(\text{radical})$, where G is the radiation chemical yield
for the given radical.

RP–HPLC. A C_4 phase reverse column $4.6 \times 150\ \text{mm}$, packed with
 $5\ \mu\text{m}$ particles (Asahipak C4P) was used. Detection was performed
using a photodiode array detector at 214 and 280 nm. The mobile
phase was delivered with a flow rate of $0.8\ \text{mL min}^{-1}$. Eluent solvents
consisted of water:acetonitrile:trifluoroacetic acid (for solvent A,
 $100:0:0.1\%$ and for solvent B, $30:70:0.1\%$ vol/vol, respectively). The
following elution program was developed: 100% of solvent A for
1 min, and then a gradient of solvent B from 0 to 100% for 70 min. All
chromatographic data acquisition was performed using the program
supplied with the Beckman system package.

Absorption and steady state fluorescence. UV–visible spectra were
performed on a Perkin Elmer Lambda 900 spectrophotometer using
1 cm path length quartz cuvettes with black side walls (Hellma). The
steady state emission and excitation spectra were recorded on a Spex
Fluorolog 1681 spectrofluorimeter using 0.3 cm path length quartz
cuvettes with black side walls (Hellma) at controlled temperature
($\pm 0.1^\circ\text{K}$). Band widths of 0.9 nm for excitation and emission were
used. Spectra were collected with integration set to 1 s and increment
of 1 nm. In all experiments, signal from buffer only was subtracted as
background. Rayleigh peaks were interpolated for clarity.

Time-resolved fluorescence. The fluorescence decay curves were
recorded at 20°C using high resolution time-correlated single photon
counting as described in (6). The excitation wavelength was 420 nm and
the fluorescence decays were measured at 474 nm. Each experimental
fluorescence decay curve $F(t)$ was analyzed individually using the
Maximum Entropy Method as described in Ref. 6. From the recovered
fluorescence lifetime distribution $a(\tau)$, the average fluorescence lifetime
 $\langle \tau_f \rangle$, is calculated as the amplitude-averaged decay time (29):

$$\langle \tau_f \rangle = \int_0^{\infty} a(\tau) \tau dt$$

Cyan fluorescent protein has been reported to undergo both reversible and irreversible slow photobleaching reactions (30). Therefore, photoreactions were carefully controlled. In time-resolved fluorescence experiments, the collection of fluorescence decays was combined to real-time monitoring of the average decay time position and intensity of the fluorescence along data acquisition. Some signal drifts were observed for [radical]/[CFP] ratios above 50 (doses higher than 450 Gy), and thus any experiment showing more than 10% intensity loss or 50 ps time-drift over the complete data acquisition was discarded. We have checked that such limited drifts resulted in undetectable modifications of the measured average fluorescence lifetime.

RESULTS AND DISCUSSION

Modification of CFP fluorescence after reaction with oxygenated free radicals

After removal of the His-tag used for protein purification, solutions of recombinant CFP were exposed to increasing doses of irradiation. Three oxidizing conditions were tested: (1) hydroxyl radical $\cdot\text{OH}$ produced in N_2O saturating conditions, (2) superoxide radical $\text{O}_2^{\cdot-}$ produced in the presence of formate ions under O_2 saturation and (3) a nearly equal mixture of both radicals obtained under air atmosphere (24). The latter condition was studied because a mixture of these two radicals closely resembles the conditions of oxidative stress (10). For each irradiated solution, the fluorescence emission spectra of CFP excited at 420 nm were compared with those of the non-irradiated sample (Fig. 1a). In all cases, a loss of fluorescence was induced by oxidation, while the shape of the spectra remained unchanged (Fig. 1b). Figure 2a shows that the relative area of the fluorescence spectra (proportional to the fluorescence quantum yield) are lowered by about 20% for a [$\cdot\text{OH}$]/[CFP] ratio of 20. This result contrasts with the report of Palazzolo *et al.* (22) who found no loss in GFP fluorescence for [$\cdot\text{OH}$]/[GFP] ratios as high as 16 000. The reason for this discrepancy is unclear, but may lie in the widely different reactivity of the different FPs toward the same oxidant (13).

At similar doses, the effect of $\text{O}_2^{\cdot-}$ on the fluorescence of CFP is less pronounced than that of $\cdot\text{OH}$ (Fig. 2a). However, the fluorescence yield variations under air, *i.e.* when a mixture of hydroxyl and superoxide radicals is produced, is as important as with $\cdot\text{OH}$ even if in these conditions only half as much $\cdot\text{OH}$ radicals are generated (Fig. 2a). Exposure of CFP to 1 mM hydrogen peroxide solution during 3 h (concentration measured by absorption, $\epsilon_{240 \text{ nm}} = 43.6 \text{ mol}^{-1} \text{ L cm}^{-1}$) (31) does not induce any modification on the fluorescence properties of a 5 μM solution of CFP. This observation is consistent with a previous report (13).

RP-HPLC analysis of the reaction products after $\cdot\text{OH}$ oxidation

The RP-HPLC chromatograms of non-irradiated CFP solutions exhibit a single peak at 40 min of elution (Fig. 3a and b). The absorption spectrum of this fraction shows a structureless chromophore band at 434 nm (Fig. 3c) characteristic of CFP at low pH (30), as expected from the acidic elution conditions

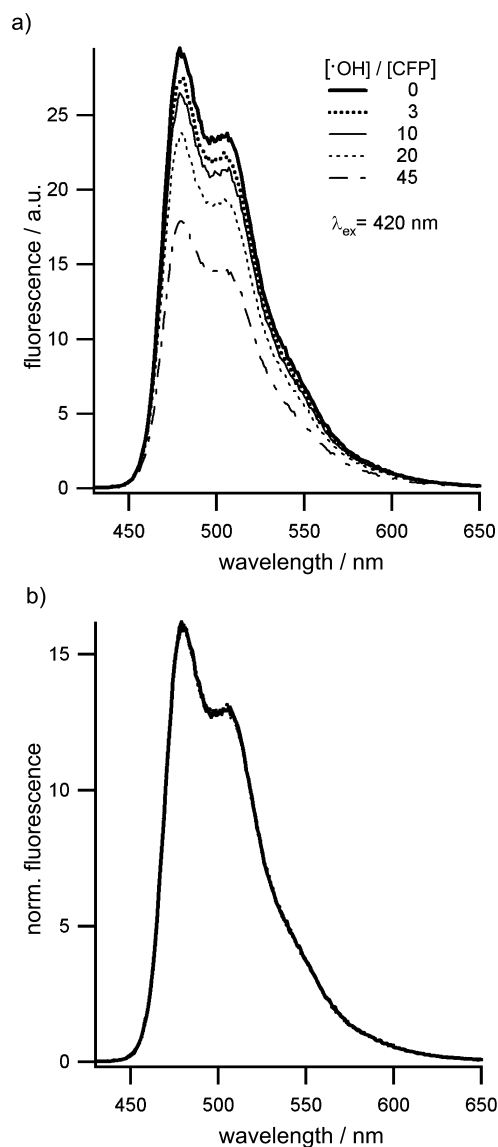


Figure 1. Representative set of fluorescence spectra of CFP solutions after oxidation by $\cdot\text{OH}$ radicals produced by γ -radiolysis (CFP 5 μM in phosphate buffer 30 mM, pH 7.4, N_2O saturated solution) recorded within the same experiment. (a) Emission spectra ($\lambda_{\text{ex}} = 420 \text{ nm}$) for increasing amounts of $\cdot\text{OH}$. These spectra, normalized *versus* their surface, are presented in (b) for a better comparison of their shape.

(see Materials and Methods). With increasing [$\cdot\text{OH}$]/[CFP] ratios, the RP-HPLC chromatograms show newly formed species eluting with a shorter retention time (note peak 2 in Fig. 3b), indicating a decreased affinity for the reversed phase material. The relative area of this new peak attributed to oxidized CFP population increases with the [$\cdot\text{OH}$]/[CFP] ratio (inset of Fig. 3b). The absorption spectrum associated with this elution peak is unchanged in the CFP chromophore region, but displays a significant increase below 350 nm (Fig. 3c). For [$\cdot\text{OH}$]/[CFP] ratios above 45, the shape of the elution peaks become poorly defined. At these high doses, after the primary oxidation of the most reactive sites of CFP, oxidation at multiple secondary sites may take place, leading to strong sample heterogeneity.

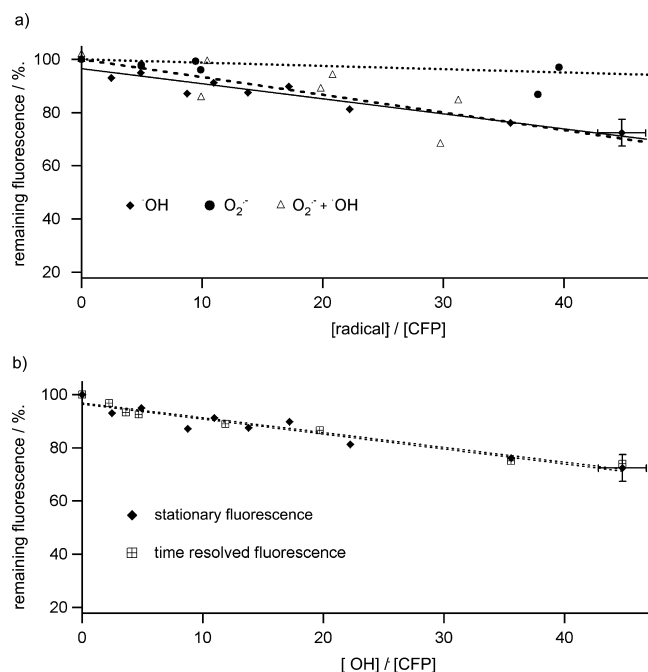


Figure 2. Comparison of the evolution of the fluorescence yield and lifetime of CFP solutions after oxidation by increasing amount of free radicals. (a) Comparison of the variation of the stationary fluorescence yield of CFP solutions after oxidation by $\bullet\text{OH}$, $\text{O}_2^{\bullet-}$ or a mixture of both. (b) Comparison of fluorescence intensities (diamond) and fluorescence lifetimes (square) for CFP oxidized by $\bullet\text{OH}$ radicals: vertical axis represent either the relative area under the fluorescence spectra ($\lambda_{\text{ex}} = 420 \text{ nm}$), or the ratio of CFP average lifetime *versus* that of nonoxidized CFP. The lines are the best linear fits of the data. Each point is an average of at least two independent experiments. Error bars are represented only on the last points for clarity.

Spectroscopic analysis of CFP solutions oxidized by $\bullet\text{OH}$ radicals

The CFP chromophore. With $[\bullet\text{OH}]/[\text{CFP}]$ ratios ≤ 45 , the chromophore absorption peak of bulk irradiated CFP samples exhibits a very similar overall shape (Fig. 4a) and an approximately constant absorbance at 434 nm (inset of Fig. 4a). Upon increasing the $[\bullet\text{OH}]/[\text{CFP}]$ ratio, the absorbance in the UV increases slightly, as observed during RP-HPLC elution. It appears to be associated to oxidized residues (32,33) in the CFP monomers rather than to scattering due to some protein aggregation. Besides, SDS-PAGE of irradiated CFP solutions (in reducing or nonreducing conditions) do not show any trace of protein oligomerization (data not shown). This rules out the formation of intermolecular covalent bonds between either cysteinyl (disulfide bonds) or tyrosinyl residues (bityrosine) in the irradiated samples. On the other hand, for a chromophore emission at 474 nm, the fluorescence excitation spectra of irradiated CFP do not show any change in shape in the CFP chromophore region nor in the UV range (Fig. 4b).

The dispersion of our absorption measurements at 434 nm does not exceed 6% in the $[\bullet\text{OH}]/[\text{CFP}]$ range 0–45 (Fig. 4a, inset), and therefore the corresponding 30% loss in fluorescence intensity (Figs. 1a and 2a) cannot be caused by an equivalent loss in absorption of the CFP chromophore. Because the shape of the emission spectra remains unchanged,

a first possibility might be that a nonfluorescent form of the chromophore is produced. If this was the case, and since this “dark” species would not contribute to the fluorescence signal, the fluorescence lifetime of the sample should remain unperturbed upon irradiation. On the contrary, the average fluorescence lifetime of oxidized CFP decreases in proportions identical to that of the stationary fluorescence intensity upon increasing $[\bullet\text{OH}]/[\text{CFP}]$ ratios (Fig. 2b).

In the presence of a molar fraction x of a “dark” population, the fluorescence intensity (proportional to the fluorescence quantum yield Φ_f) and the fluorescence lifetime τ_f are linked through the following relationship (29):

$$\Phi_f = (1 - x) \frac{k_r}{k_r + k_{nr}} = (1 - x)k_r\tau_f,$$

where k_r is the chromophore radiative rate and k_{nr} the sum of all nonradiative rates contributing to chromophore dynamic quenching. The parallel decrease in fluorescence lifetime and intensity shows that, under the conditions used, CFP oxidation does not lead to the formation of a “dark” chromophore. Instead, the CFP chromophore shows a decreased fluorescence quantum yield and lifetime but retains mostly unchanged intrinsic electronic properties (k_r remains unaffected), showing that it is not directly chemically modified. The observed fluorescence perturbations reflect most probably modifications of the chromophore nearby interactions, leading to an increased overall efficiency of dynamic quenching through nonradiative de-excitation paths (k_{nr}).

The case of tryptophan 57. There is only one tryptophanyl residue in the CFP sequence and *ca.* 97 % of its fluorescence is quenched *via* FRET by the chromophore ($d[\text{W}^{57}\text{-chromophore}] = 17 \text{ \AA}$) (34). As a result, for an excitation at 280 nm, its direct emission at 340 nm is barely detectable, and the fluorescence of tyrosinyl residues around 310 nm is unmasked (Fig. 5a, bold curve). A strong emission of the CFP chromophore is observed instead at 474 nm, which results both from energy transfer from W^{57} and from direct CFP chromophore excitation into a higher electronic absorption band (34). After oxidation up to a $[\bullet\text{OH}]/[\text{CFP}]$ ratio of 20, the emission spectra excited at 280 nm do not change between 300 and 400 nm, while the chromophore emission at 474 nm decreases (Fig. 5a). Moreover, the percentage of remaining chromophore fluorescence *versus* the non-irradiated sample is identical under either direct (420 nm) or indirect (280 nm) excitation (Fig. 5b), which is also consistent with the unchanged chromophore excitation spectra of Fig. 4b.

We can therefore conclude that the photophysical properties of W^{57} as well as its energy transfer interaction with the CFP chromophore are not modified by $\bullet\text{OH}$ radical oxidation. Thus the oxidation of W^{57} by $\bullet\text{OH}$ radicals is very unlikely. Besides, this result is a strong indication of a good preservation of the overall protein structure, since it implies that all photophysical, structural and dynamic determinants of the energy transfer process remain unchanged. For example, assuming all other parameters constant, an increase of 0.6 Å in the distance between W^{57} and the CFP chromophore would have resulted in a 20 % variation in the fluorescence intensity observed at 340 nm, a modification that would certainly not have escaped detection. Therefore, we can rule out any

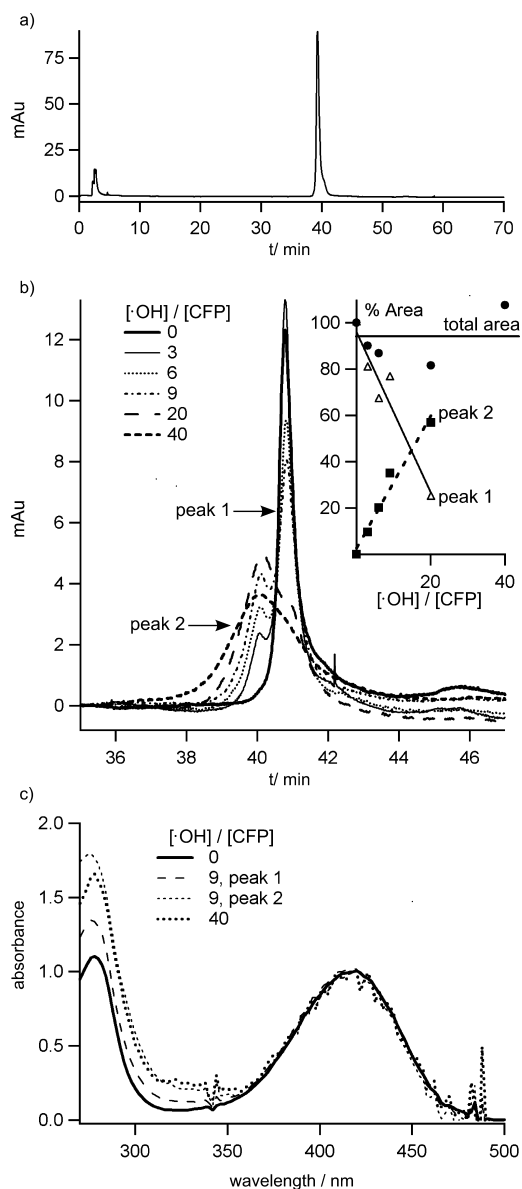


Figure 3. (a) HPLC chromatogram of CFP ($5 \mu\text{M}$) for a detection at 280 nm. (b) Evolution of the HPLC chromatogram with increasing amounts of $\cdot\text{OH}$. The inset represents the variations in total area and that of the first and second peaks. (c) Normalized absorption spectra (versus their maximum of absorbance) recorded by the HPLC system at the chromatogram's maximum for 0, 9 and 40 $[\cdot\text{OH}]/[\text{CFP}]$ ratios.

significant denaturation or cleavage of the CFP protein after γ -irradiation.

CONCLUSION

The CFP sensitivity to $\cdot\text{OH}$ suggests an oxidation mechanism that differs notably from the previously described direct oxidative destruction of the GFP chromophore by hypochlorous acid (22). Here, radical oxidation leads to new fluorescent properties of an otherwise chemically intact CFP chromophore. These perturbations may arise from the specific oxidation of nearby residue(s) in the protein. It is also possible that CFP chemical modifications lead to a decreased stiffness

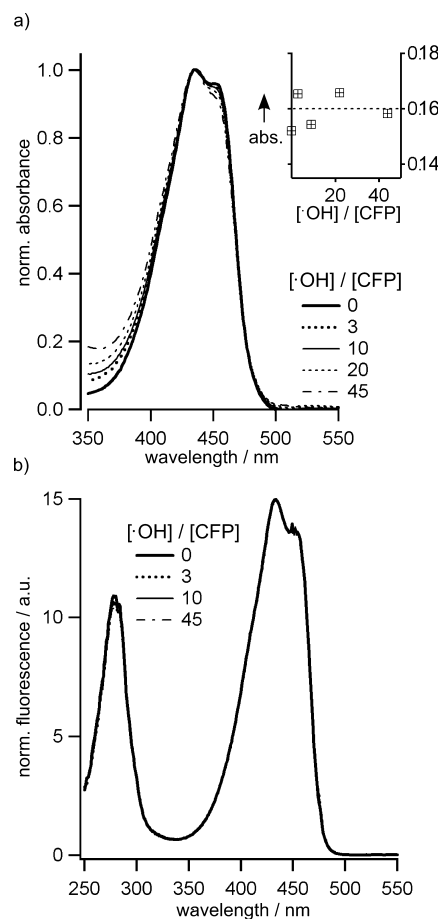


Figure 4. (a) Representative set of UV-visible absorption spectra of CFP solutions after oxidation by $\cdot\text{OH}$, normalized versus their absorption at 434 nm. The inset represents the variation of the absolute absorbance at $\lambda = 434 \text{ nm}$ as a function of the ratio $[\cdot\text{OH}]/[\text{CFP}]$ for the same spectra set. (b) CFP excitation spectra ($\lambda_{\text{em}} = 474 \text{ nm}$) for increasing amounts of $\cdot\text{OH}$ normalized versus their surface between 350 and 550 nm.

of the chromophore pocket, allowing a higher rate of excited state torsions, which is a major quenching process in FP chromophores (35). This idea is supported by the analogous effects of ROS and increasing temperatures in CFP, *i.e.* a strong decrease in average lifetime and quantum yield without major modifications or shift of the chromophore emission spectrum (6). Interestingly also, the direct photo-products of CFP, as obtained during cell microscopy imaging, similarly display a decreased fluorescence lifetime without noticeable change of their emission spectrum (25). The chemical nature of the ROS produced during photochemical reactions in CFP is still a matter of debate. Nevertheless, it could be expected that ROS-induced production of weaker fluorescent forms of CFP will take place in all situations of intense illumination, for example after the thorough photobleaching of its nearby YFP acceptor, which adds one more viewpoint in the current debate on the unreliability of this popular technique (see 36, 37 and references cited therein). However, the chemical and photophysical consequences of ROS exposure may vary strongly with the dose, the specific oxidant and the FP variant. Many chemical imaging techniques require an accurate comparison of fluorescence inten-

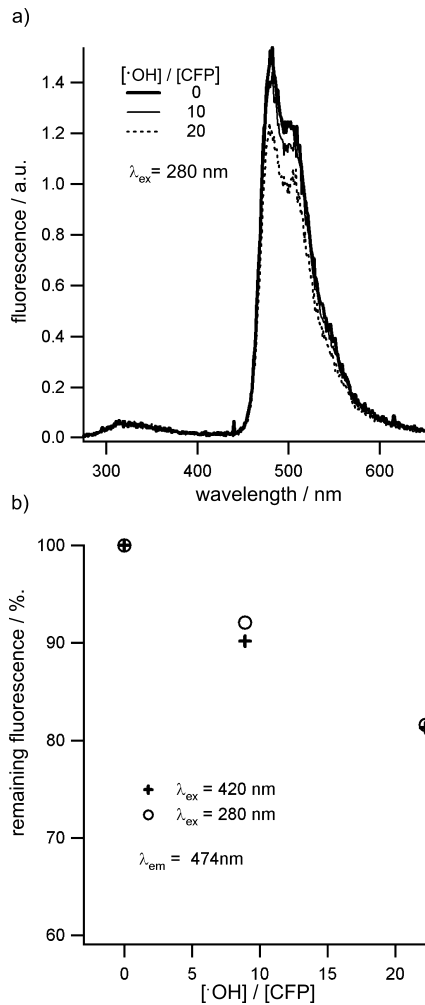


Figure 5. Observation of FRET between the W⁵⁷ and the CFP chromophore. (a) Emission spectra ($\lambda_{\text{ex}} = 280 \text{ nm}$) for increasing amounts of $\bullet\text{OH}$. (b) Evolution of the percentage of remaining fluorescence at 474 nm for two excitation wavelengths 280 and 420 nm versus that of the non-irradiated solution. Fluorescence spectra of CFP solutions after oxidation by $\bullet\text{OH}$ radicals.

sities or lifetimes within a few percents. It is indeed technically possible to measure routinely fluorescence lifetimes within the cellular environment with accuracies better than 1 % (36). Within this frame, the demonstrated CFP sensitivity to $\bullet\text{OH}$ should be taken into account. Strict controls *in situ* will be required when this FP is to be used in situations of oxidative activity (phagocytosis, mitochondrial activity, apoptosis and inflammation), especially in the numerous cases where the exact amount and the chemical nature of the produced ROS remains mostly unknown.

Detailed structural analyses of CFP using mass spectrometry (38) are being applied to its oxidation products, which should provide further insight into its structure–photophysics relationships, as well as on the oxidation mechanisms that take place.

Acknowledgements—This work was supported by CNRS, Paris-Sud 11 University, the Fondation pour la Recherche Medicale (FRM), and an ACI from FNS-MENESR (DRAB). Luis Alvarez was supported by a thesis grant from the French Ministry of Research. Chantal Houé Levin acknowledges the COST CM0603 for fruitful discussions.

REFERENCES

- Shaner, N. C., G. H. Patterson and M. W. Davidson (2007) Advances in fluorescent protein technology. *J. Cell Sci.* **120**, 4247–4260.
- Prinz, A., G. Reither, M. Diskar and C. Schultz (2008) Fluorescence and bioluminescence procedures for functional proteomics. *Proteomics* **8**, 1179–1196.
- Zhang, J., R. E. Campbell, A. Y. Ting and R. Y. Tsien (2002) Creating new fluorescent probes for cell biology. *Nat. Rev. Mol. Cell Biol.* **3**, 906–918.
- Bizzarri, R., R. Nifosi, S. Abbruzzetti, W. Rocchia, S. Guidi, D. Arosio, G. Garau, B. Campanini, E. Grandi, F. Ricci, C. Viappiani and F. Beltram (2007) Green fluorescent protein ground states: The influence of a second protonation site near the chromophore. *Biochemistry* **46**, 5494–5504.
- Shu, X., K. Kallio, X. Shi, P. Abbyad, P. Kanchanawong, W. Childs, S. G. Boxer and S. J. Remington (2007) Ultrafast excited-state dynamics in the green fluorescent protein variant S65T/H148D. I. Mutagenesis and structural studies. *Biochemistry* **46**, 12005–12013.
- Villoing, A., M. Ridhoir, B. Cinquin, M. Erard, L. Alvarez, G. Vallverdu, P. Pernot, R. Grailhe, F. Merola and H. Pasquier (2008) Complex fluorescence of the cyan fluorescent protein: Comparisons with the H148D Variant and consequences for quantitative cell imaging. *Biochemistry* **47**, 12483–12492.
- Arosio, D., G. Garau, F. Ricci, L. Marchetti, R. Bizzarri, R. Nifosi and F. Beltram (2007) Spectroscopic and structural study of proton and halide ion cooperative binding to GFP. *Biophys. J.* **93**, 232–244.
- Wachter, R. M., D. Yarbrough, K. Kallio and S. J. Remington (2000) Crystallographic and energetic analysis of binding of selected anions to the yellow variants of green fluorescent protein. *J. Mol. Biol.* **301**, 157–171.
- Van Manen, H. J., P. Verkuijlen, P. Wittendorp, V. Subramaniam, T. K. van den Berg, D. Roos and C. Otto (2008) Refractive index sensing of green fluorescent proteins in living cells using fluorescence lifetime imaging microscopy. *Biophys. J.* **94**, L67–L69.
- Aruoma, O. I. and B. Halliwell (1998) *Molecular Biology of Free Radicals in Human Diseases*. OICA International, London.
- Hoppe, A. D. and J. A. Swanson (2004) Cdc42, Rac1, and Rac2 display distinct patterns of activation during phagocytosis. *Mol. Biol. Cell* **15**, 3509–3519.
- Ueyama, T., T. Tatsuno, T. Kawasaki, S. Tsujibe, Y. Shirai, H. Sumimoto, T. L. Leto and N. Saito (2007) A regulated adaptor function of p40^{phox}: Distinct p67^{phox} membrane targeting by p40^{phox} and by p47^{phox}. *Mol. Biol. Cell* **18**, 441–454.
- Tsourkas, A., G. Newton, J. M. Perez, J. P. Basilion and R. Weissleder (2005) Detection of peroxidase/H₂O₂-mediated oxidation with enhanced yellow fluorescent protein. *Anal. Chem.* **77**, 2862–2867.
- Wang, W., H. Q. Fang, L. Groom, A. W. Cheng, W. R. Zhang, J. Liu, X. H. Wang, K. T. Li, P. D. Han, M. Zheng, J. H. Yin, W. D. Wang, M. P. Mattson, J. P. Y. Kao, E. G. Lakatta, S. S. Sheu, K. F. Ouyang, J. Chen, R. T. Dirksen and H. P. Cheng (2008) Superoxide flashes in single mitochondria. *Cell* **134**, 279–290.
- Gutscher, M., A. L. Pauleau, L. Marty, T. Brach, G. H. Wabnitz, Y. Samstag, A. J. Meyer and T. P. Dick (2008) Real-time imaging of the intracellular glutathione redox potential. *Nat. Methods* **5**, 553–559.
- Lohman, J. R. and S. J. Remington (2008) Development of a family of redox-sensitive green fluorescent protein indicators for use in relatively oxidizing subcellular environments. *Biochemistry* **47**, 8678–8688.
- Calzavara-Pinton, P. G., M. Venturini and R. Sala (2007) Photodynamic therapy: Update 2006—Part 1: Photochemistry and photobiology. *J. Eur. Acad. Dermatol.* **21**, 293–302.
- Bulina, M. E., K. A. Lukyanov, O. V. Britanova, D. Onichtchouk, S. Lukyanov and D. M. Chudakov (2006) Chromophore-assisted light inactivation (CALI) using the phototoxic fluorescent protein KillerRed. *Nat. Protocols* **1**, 947–953.
- Fernandez-Suarez, M. and A. Y. Ting (2008) Fluorescent probes for super-resolution imaging in living cells. *Nat. Rev. Mol. Cell Biol.* **9**, 929–943.

- 1 20. Bou-Abdallah, F., N. D. Chasteen and M. P. Lesser (2006)
2 Quenching of superoxide radicals by green fluorescent protein.
3 *Biochim. Biophys. Acta* **1760**, 1690–1695.
- 4 21. Espey, M. G., S. Xavier, D. D. Thomas, K. M. Miranda and
5 D. A. Wink (2002) Direct real-time evaluation of nitration with
6 green fluorescent protein in solution and within human cells
7 reveals the impact of nitrogen dioxide vs. peroxynitrite mecha-
8 nisms. *Proc. Natl Acad. Sci. USA* **99**, 3481–3486.
- 9 22. Palazzolo, A. M., C. Suquet, M. E. Konkel and J. K. Hurst (2005)
10 Green fluorescent protein-expressing *Escherichia coli* as a selective
11 probe for HOCl generation within neutrophils. *Biochemistry* **44**,
12 6910–6919.
- 13 23. Piston, D. W. and G. J. Kremers (2007) Fluorescent protein
14 FRET: The good, the bad and the ugly. *Trends Biochem. Sci.* **32**,
15 407–414.
- 16 24. Spinks, J. W. T. and R. J. Woods (1990) *Introduction to Radiation*
17 *Chemistry*. Wiley Interscience, New York.
- 18 25. Tramier, M., M. Zahid, J. C. Mevel, M. J. Masse and M. Coppey-
19 Moisan (2006) Sensitivity of CFP/YFP and GFP/mCherry pairs
20 to donor photobleaching on FRET determination by fluorescence
21 lifetime imaging microscopy in living cells. *Microsc. Res. Tech.* **69**,
22 933–939.
- 23 26. Kapust, R. B., J. Tozser, J. D. Fox, D. E. Anderson, S. Cherry,
24 T. D. Copeland and D. S. Waugh (2001) Tobacco etch virus protease:
25 Mechanism of autolysis and rational design of stable mutants
26 with wild-type catalytic proficiency. *Protein Eng.* **14**, 993–1000.
- 27 27. Cubitt, A. B., L. A. Woollenweber and R. Heim (1999) Under-
28 standing structure-function relationships in the *Aequorea victoria*
29 green fluorescent protein. *Methods Cell Biol.* **58**, 19–30.
- 30 28. Mozziconacci, O., J. Mirkowski, F. Rusconi, P. Pernot,
31 K. Bobrowski and C. Houée-Levin (2007) Superoxide radical
32 anions protect enkephalin from oxidation if the amine group is
33 blocked. *Free Radic. Biol. Med.* **43**, 229–240.
- 34 29. Valeur, B. (2006) *Molecular Fluorescence. Principles and Applica-*
35 *tions*. Wiley-VCH, Weinheim.
- 36 30. Sinnecker, D., P. Voigt, N. Hellwig and M. Schaefer (2005)
37 Reversible photobleaching of enhanced green fluorescent proteins.
38 *Biochemistry* **44**, 7085–7094.
- 39 31. Rota, C., C. F. Chignell and R. P. Mason (1999) Evidence for free
40 radical formation during the oxidation of 2'-7'-dichlorofluorescein
41 to the fluorescent dye 2'-7'-dichlorofluorescein by horseradish
42 peroxidase: Possible implications for oxidative stress measure-
43 ments. *Free Radic. Biol. Med.* **27**, 873–881.
- 44 32. Bartolome, B., M. L. Bengoechea, M. C. Galvez, F. J.
45 Perezilzarbe, T. Hernandez, I. Estrella and C. Gomezcordoves
46 (1993) Photodiode-array detection for elucidation of the structure
47 of phenolic-compounds. *J. Chromatogr. A* **655**, 119–125.
- 48 33. Zegota, H., K. Kolodziejczyk, M. Krol and B. Krol (2005)
49 *o*-Tyrosine hydroxylation by OH center dot radicals. 2,3-DOPA
50 and 2,5-DOPA formation in gamma-irradiated aqueous solution.
51 *Rad. Phys. Chem.* **72**, 25–33.
- 52 34. Visser, N. V., J. W. Borst, M. A. Hink, A. van Hoek and A. Visser
53 (2005) Direct observation of resonance tryptophan-to-chromo-
54 phore energy transfer in visible fluorescent proteins. *Biophys.*
55 *Chem.* **116**, 207–212.
- 56 35. Maddalo, S. L. and M. Zimmer (2006) The role of the protein
57 matrix in green fluorescent protein fluorescence. *Photochem.*
58 *Photobiol.* **82**, 367–372.
- 59 36. Grailhe, R., F. Merola, J. Ridard, S. Couvignou, C. Le Poupon,
60 J. P. Changeux and H. Laguitton-Pasquier (2006) Monitoring
61 protein interactions in the living cell through the fluorescence
decays of the cyan fluorescent protein. *Chemphyschem* **7**, 1442–
1454.
37. Kirber, M. T., K. Chen and J. F. Keaney (2007) YFP photo-
conversion revisited: Confirmation of the CFP-like species. *Nat.*
Methods **4**, 767–768.
38. Alvarez, L. A., F. Merola, M. Erard and F. Rusconi (2009) Mass
spectrometry-based structural dissection of fluorescent proteins.
Biochemistry **48**, 3810–3812.

Author Query Form

Journal: PHP

Article: 617

Dear Author,



During the copy-editing of your paper, the following queries arose. Please respond to these by marking up your proofs with the necessary changes/additions. Please write your answers on the query sheet if there is insufficient space on the page proofs. Please write clearly and follow the conventions shown on the attached corrections sheet. If returning the proof by fax do not write too close to the paper's edge. Please remember that illegible mark-ups may delay publication.

Many thanks for your assistance.

Query reference	Query	Remarks
1	AUTHOR: This article has been lightly edited for grammar, style and usage. Please compare it with your original document and make changes on these pages. Please limit your corrections to substantive changes that affect meaning. If no change is required in response to a question, please write "OK as set" in the margin. Copy editor.	
2	AUTHOR: Please define DsRed.	
3	AUTHOR: Please define PMSF.	
4	AUTHOR: 40 000 rpm: please replace this with the correct <i>g</i> value.	
5	AUTHOR: Please define NTA.	
6	AUTHOR: Please define DTT.	
7	AUTHOR: Please define TEV.	
8	AUTHOR: Please provide the appropriate section heading in place of the text "see below."	
9	AUTHOR: Supporting Information has been cited in the text. Please forward the necessary files to the Production Editor so that they can appear online with your paper.	

Proof Correction Marks

Please correct and return your proofs using the proof correction marks below. For a more detailed look at using these marks please reference the most recent edition of The Chicago Manual of Style and visit them on the Web at: <http://www.chicagomanualofstyle.org/home.html>

<i>Instruction to typesetter</i>	<i>Textual mark</i>	<i>Marginal mark</i>
Leave unchanged	... under matter to remain	<i>stet</i>
Insert in text the matter indicated in the margin	^	^ followed by new matter
Delete	Ʒ through single character, rule or underline or Ʒ through all characters to be deleted	<i>e</i>
Substitute character or substitute part of one or more word(s)	Ƶ through letter or — through characters	new character Ƶ or new characters Ƶ
Change to italics	— under matter to be changed	<i>ital</i>
Change to capitals	≡ under matter to be changed	<i>Caps</i>
Change to small capitals	≡ under matter to be changed	<i>sc</i>
Change to bold type	~ under matter to be changed	<i>bf</i>
Change to bold italic	~ under matter to be changed	<i>bf+ital</i>
Change to lower case	Ɔ	<i>lc</i>
Insert superscript	√	√ under character e.g. √
Insert subscript	^	^ over character e.g. ^
Insert full stop	⊙	⊙
Insert comma	↗	↗
Insert single quotation marks	↙ ↘	↙ ↘
Insert double quotation marks	↖ ↗	↖ ↗
Insert hyphen	=	=
Start new paragraph	¶	¶
Transpose	┌┐	┌┐
Close up	linking  characters	
Insert or substitute space between characters or words	#	#
Reduce space between characters or words	⌒	⌒